POLITECNICO
MILANO 1863

SCUOLA DI INGEGNERIA INDUSTRIALE
E DELL'INFORMAZIONE

Executive Summary of the Thesis

Production cycle optimization for pumping airborne wind energy systems

Laurea Magistrale in Automation and Control Engineering - Ingegneria dell'Automazione

Author: Rodolfo Mathis

Advisor: Prof. Lorenzo Mario Fagiano

Academic year: 2021-22

1. Introduction

It is widely established that one of the biggest challenges of the 21st century is finding a solution to the problem of energy supply and production. For this reason many new technology are rising in the renewable energy field. System Airborne Wind Energy (AWE) is a fascinating technology to convert wind power into electricity with an autonomous tethered aircraft. AWE is a technology that is still in its infancy and it is aiming for deployment in a variety of markets and applications. Therefore many technology approaches, concepts of operation, and designs are under consideration.
This thesis describes an approach to increase the efficiency of an AWE system with soft wing flying in crosswind motion. In those systems the power generation occurs in cycles, each consisting of a productive *Traction* phase where the cable is unwound and a consuming phase called *Retraction* where the cable is rewound. Transition phases are required to go from the *Traction* phase to the *Retraction* phase (*Transition 1* or shortly $T1$) and vice versa (*Transition 2*).
In the present work, the problem was first addressed by increasing the efficiency of *Transition 1* and then through full-cycle optimization. Two ideas guided this work: one is to implement a control logic that guarantees a smooth transient behavior for the forces acting on the tether ensuring the maximum lifetime of the components; the other is to maximize the average cycle power production that is the key aspect of any energy production system. More in detail, an optimal elevation-azimuth trajectory for the *Transition 1* at varying wind speed are found, the optimal solution take into account also the optimality of the *Traction* and *Retraction* phases through the reeling velocities. Concerning the transition phase, two different control strategies that avoid abrupt increase in the force acting on the tether were implemented. The first one exploits the measure of the wind and ensures that the winch controller follows the desired reeling speed profile. The second implementation does not rely on wind measurements, which are often unreliable and not suitable for real world applications.

1.1. Cycle basic operating principles

In order to better understand how does the pumping AWE system work, let's briefly intro-

duce the basic operating principles. The kite flies as it is blown by the wind and applies tension on the tether. The unreeling of the tether from the drum produces a rotational motion that is transformed into electrical energy using a generator. The duty cycle is composed of four phases:

TRACTION: During this phase the energy is produced, the tether is reeled out while high forces are acting on the sail.

TRANSITION 1: This phase manages the kite's transition out of wind.

RETRACTION: Energy is used to retract the cable to enable the start of a new cycle. This operation is done while the kite is positioned out of the wind such that less energy is used to reel-in than what was produced during the *Traction*.

TRANSITION 2: After the tether is completely reeled in, this phase ensure that the kite position is the one desired to be able to start the next productive cycle.

The switching conditions between one phase and the next are a sensitive parameter that influence the system overall stability and safety.

2. System Modelling

To give a short description, of a pumping AWE system we can say that it consists of the kite's sail and a tether (or two tethers, depending on the kite model) that links it to the ground station. At the ground station, the cable is operated by a winch that is connected to a generator through a gearbox to produce electrical energy. The Awe system considered here has just one tether and the maneuvering (steering) actuation system is placed on a unit at the end of the tether (SU: steering unit); from the SU two pairs of cables exit and connect to the two sides of the wing. Modelling the wing as a point-mass, a dynamic model of the AWE system based on first principles was considered [2]. The kite position is expressed in spherical coordinates as a function of its distance from the origin r, of the elevation angle θ and the azimuth angle φ. The dynamic model of the kite's motion can be derived applying Newton's laws. The forces that have been considered in the modelling include the contributions of gravity force F_{grav} (of the kite and the tether), the apparent force F_{app}, the aerodynamic force F_{aer} and traction force F_{tr} due to the interaction with the tether.

In this work, the tether model developed in [1] is adopted. This consists of a multi-body modellization of the tether that is discretized in segments and its mass split into N point mass nodes; each segments is modelled as a spring-damper system. Points at the extremes of the tether are added to take into account the presence of the kite and the ground station; each inner node is subject to its own weight, to the aerodynamic force, and to the forces applied by the two neighboring tether segment.

The ground station handles the tether and converts mechanical power to electrical power. Its main components are a winch drum, a gearbox, an electric drives able to act either as generators or as motors and a converter. In addition, power electronics for grid connection and/or battery storage system are present.

After having modelled the different components of the system, their design has been discussed and their characteristic parameters has been set.

3. Control Structure

On the ground level, to manage the tether reeling-in and reeling-out operation there is the "winch-engines" unit system, while the sail flying trajectory is controlled by the KSU. The tether is connecting the two subsystems and allows the force transfer accordingly to the elastic damped model. This structure allows for a decoupled control structure for the reeling speed and the flight "trajectory". The quotation marks want to highlight that the term trajectory is used here and in the following sections to indicate the azimuth-elevation displacement of the kite.

3.1. Trajectory control

To control the kite during flight, two different control trajectory strategies has been developed: one is based on the concept of velocity angle and is used to fly the kite during the *Traction* phase and the two *Transition* phases, while the second one generates the steering angle based only on the reference values of the elevation angle θ. The velocity angle is defined by the following equation:

$$\gamma(k) = \arctan\left(\frac{\cos(\theta(k))\dot{\varphi}(k)}{\dot{\theta}(k)}\right)$$

and it has been introduced in [3] so to suitably control the steering of the wing.
The main control structure during *Traction* phase consists in a cascade control composed by two control loops (see [3]): the outer one is responsible for the trajectory tracking of the kite while the inner loop provides the control steering commands. This control system has been suitably designed for the generation of the eight paths. The second controller is based on the tracking of the θ angle, this controller is used only during the *Retraction* phase when the kite is in steady state angular position at the border of wind window. It consists in a cascaded control where the outer loop is responsible for the generation of the desired reference trajectory while the inner loop block, a standard PID controller, generates the proper steering command.

3.2. Winch control

As previously described, the kite system alternates between reel-in and reeling-out phases to produce energy. The following equation in the Laplace domain, links the tether length to the torques provided by the engine to the traction exerted by the kite.

$$l_t(s) = \frac{\frac{r_d}{n}}{J_{tot}s^2 + c_{f_{tot}}s} T_m(s) + \frac{(\frac{r_d}{n})^2}{J_{\text{tot}}s^2 + c_{f_{\text{tot}}}s} F_t(s)$$

in the equation above, T_m is the torque on the engine side and F_t is the tether force applied at the winch, while n is the gearbox ratio, r_d is the drum radius, J_{tot} is the total moment inertia and the $c_{f_{tot}}$ is the total viscous friction coefficient of the engine drum group.
To control the reeling speed v of the tether a standard PI Controller as been introduced (see figure 1). In figure 1 v_{ref} is the reeling speed set point. To prevent windup phenomena due to saturation of the actuator, a proper anti-windup scheme has been adopted.

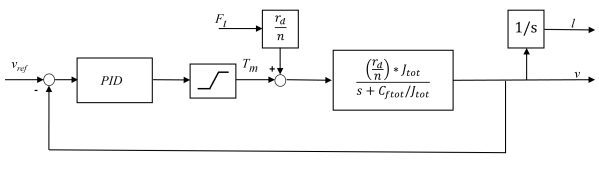

Figure 1: Winch system closed loop control system

3.3. Supervisory controller

The kite during its operational cycle, switches between different phases (*Traction, Transition 1, Retraction* and *Transition 2*) each characterized by a different control structure and/or control parameters. To handle this, a supervisory controller has been developed and suitable switching conditions have been designed. Choosing good switching condition between phases is crucial for the good behavior and robustness of the system.
In order to prevent the occurrence of windup effects due to the fact that the PID controllers are alternatively activated, a suitable logic has been implemented so to perform what is called "integral tracking".

4. Cycle Optimization

The main contributions of this work are the implementation of a control logic that ensure the absence of force spikes on the tether during the *Transition 1* and the optimization of the kite's trajectory during this transient.

4.1. Winch control strategy

Before introducing the control logic implemented, let's recall one important consideration: at the beginning of the *Transition 1* the kite is downwind and during the transition it flies out of the wind. This implies, if the reeling speed doesn't change, that the force decreases. Taking that into account, the idea was to decrease the reeling speed as much as it would not cause an abrupt increase in the tether force. To do so, the first strategy uses the following formula in order to compute the reeling speed reference:

$$v_{ref} = W cos(\theta) cos(\varphi) - \sqrt{\frac{F_{t,ref}}{C}}$$

where W is the wind speed and $F_{t,ref}$ is the desired force for the *Transition 1*, chosen as the tether force value measured at the end of the *Traction* phase.
Due to the limited accuracy, wind speed cannot be used as a feedback variable by the winch controller, which is the major drawback that limits potential real world applicability of this strategy. This lead to the implementation of the next approach.

The second approach succeeds in overcoming the lack of wind speed measurement. The mechanical torque T_m on the engine side at the switching instant between the *Traction* phase and the *Transition 1* is measured and its value is then used to limit the control action during the entire transition (see algorithm 1).
The reference speed v_{ref} is set equal to the one of the *Retraction* phase. Since at the beginning of the *Transition 1* the actual value of the reeling speed is far from it, this causes the controller to generate a high torque request to the actuator. The saturation value imposed, severely limits the actual actuator torque guaranteeing the desired smooth force trend.

Algorithm 1 Winch Supervisor Logic

1: **if** $Start_{T1} = True$ **then**
2: $T_{m,\max} = T_m(k)$
3: **end if**
4: **if** $phase = Transition\ 1$ **then**
5: $v_{\text{ref}}(k) = v_{\text{retraction}}$
6: **end if**

Looking at the control scheme in figure 1, it can be noticed that by imposing the artificial saturation to the control action and giving a reference speed that saturate it, the system is basically an open-loop system whose output depends only on the disturbance F_t. From a control point of view this would clearly seems as a mistake. However from a practical point of view the controller's inability to compensate for an increase in the disturbance is acceptable or rather desirable: a sudden rise of the disturbance F_t (e.g. a gust of wind) would lead to reel-out some extra meters of cable instead of exposing it to high stress.

4.2. Optimization problem

The nonlinear trajectory optimization problem aim to find the four optimal target points Q_{t1} and the optimal reeling speeds v_{reel} that maximises the average power production at different wind speed. In order to easily compare the results obtained, the switching condition for the start of the *Transition 1* has been chosen to ensure that the kite is always in the same location of the eight-figure path.
Since we are dealing with a quite complex-nonlinear problem some constraints are added in order to find the desired solution. Linear constraint on the target point elevation and azimuth angle have been added to ensure they are sequentially used and that their values is confined in a reasonable range. The reeling velocity have also been limited in range. Moreover a nonlinear constraint on the maximum force has be added to ensure that the forces acting on the kite are below the desired limit.
In the cost function the average power P_{avg} is maximised and its values is computed as:

$$P_{\text{avg}} = \frac{1}{T}\sum_{k=0}^{T} T_{m_k}(Q_{t1}, v_{\text{reel}})\omega_{m_k}(Q_{t1}, v_{\text{reel}})$$

Then the optimization problem can be written as follows:

$$\max_{Q_{t1}, v_{reel}} \; P_{avg}(Q_{t1}, v_{reel})$$

s.t.

$$\begin{aligned}
0.3 \le \theta_i \le 1 \quad & \text{with } i = 1 \dots N-1 \\
\theta_i \le \theta_{i+1} \quad & \text{with } i = 1 \dots N-1 \\
\theta_{ref_{t1}} \le \theta_N \le \frac{\pi}{2} & \\
-\frac{\pi}{2} \le \varphi_i \le \frac{\pi}{2} \quad & \text{with } i = 1 \dots N \\
\varphi_i \le \varphi_{i+1} \quad & \text{with } i = 1 \dots N-1 \\
0 \le v_{\text{traction}} \le v_{\text{traction,MAX}} & \\
v_{\text{retraction,MIN}} \le v_{\text{retraction}} \le 0 & \\
F_t(Q_{t1}, v_{\text{reel}}) \le \frac{F_{\text{tether,MAX}}}{c_{s,t}} &
\end{aligned}$$

5. Simulation results

First of all, let's introduce the benchmark approach that will be used in the next pages to evaluate the solutions presented (see figure 2).

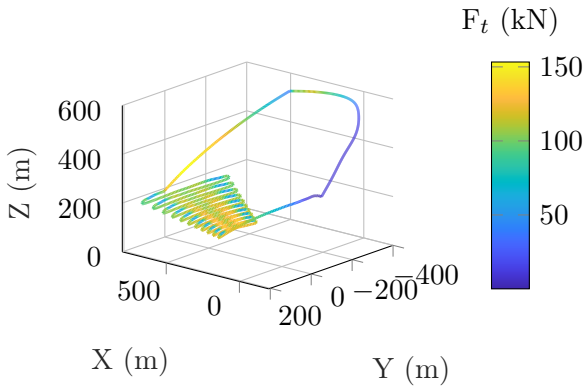

Figure 2: Kite's 3-dimensional trajectory corresponding to the benchmark approach, the force acting on the tether is color coded

The benchmark is obtained by running the simulation with the following conditions. For the *Transition 1* the reeling reference speed for the $T1$ is imposed equal to 0 and a unique target point is used to fly the kite out of wind. For the *Traction* and the *Retraction* phase the optimized reeling reference speed are used, doing so ensures that the results presented are not biased by this sensitive choices.

5.1. Controller results

The performance of the two control logic implemented are here compared to the benchmark approach. In figure 3 a satisfactory behaviour of F_t is shown from both the implemented controllers, while the benchmark approach shows an elevated force peak. With the proposed solutions the components lifetime, especially the cable one's, are maximised.
The kite is quickly and efficiently moved from being downwind, unwinding the tether, to the edge of the wind power zone already reeling in the cable. In this situation the *Retraction* phase can smoothly start.

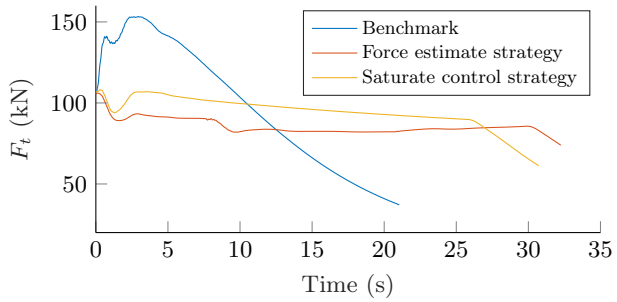

Figure 3: Comparison of force acting on the tether during the *Transition 1* with the original winch control implementation, the so called "force estimate strategy" and the "saturated control strategy".

5.2. Optimal Trajectory

The optimal solution found by the algorithm at wind speed $W = 12\,\mathrm{m\,s^{-1}}$ imposes the reference reeling speed values for the *Traction* and the *Retraction* equal to $2.7\,\mathrm{m\,s^{-1}}$ and $-4.7\,\mathrm{m\,s^{-1}}$, respectively. The trajectory is described by the four optimal target points found by the routine that are listed in the table 1.

	θ	φ
1	0.3156	0.1848
2	0.4761	0.7933
3	0.7821	0.8531
4	1.0823	1.5708

Table 1: Optimal target points

To quantify the improvement achieved by following the optimal trajectory, the average cycle power was compared with a baseline approach where the $T1$ trajectory is described by one unique target point and the reference reeling speed of the tether is kept equal to zero during the entire transition. The proposed optimized cycle achieves an average cycle power increase of approximately of 3.7% as can be seen in the last column of table 3.

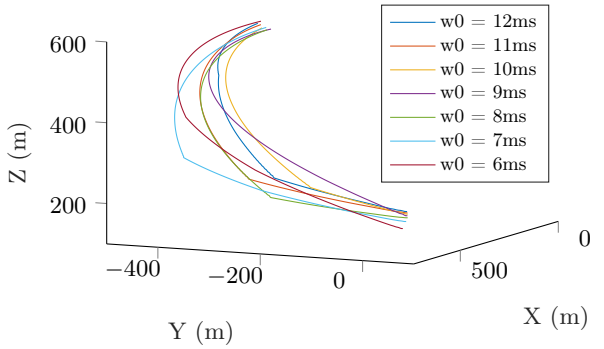

Figure 4: Optimal *Transition 1* trajectory at varying wind speed.

Once the solution was proved successful the optimization routine was performed several times by varying the wind intensity from $12\,\mathrm{m\,s^{-1}}$ down to $6\,\mathrm{m\,s^{-1}}$.
The obtained trajectory shown in figure 4 highlights that the trajectory followed by the kite are all similar for in the entire wind range, that lead to the idea of finding one unique sequence of target points that could be use independently from the wind speed. The term "sub-optimal solution" will be used to refer to such solution. The target points used are reported in table 2.

	θ	φ
1	0.3608	0.7625
2	0.4508	1.0210
3	0.7822	1.1670
4	1.0621	1.5353

Table 2: Average of the optimal target points for $W \in [6, 12]$ [m/s]

The comparison of the average power production obtained in the optimal and sub-optimal case at the varying wind speed are shown in the following table. Moreover, the 3-dimentional trajectories of *Transition 1* obtained with the sub-optimal solution are shown in the figure 5 .

Wind speed W [m/s]	6	7	8	9	10	11	12
Benchmark [kW]	11.71	20.07	34.30	48.50	66.93	87.81	114.88
Optimal [kW]	13.46	21.78	35.12	49.68	68.65	91.26	119.09
% increase	14.9%	8.5%	2.4%	2.4%	2.6%	3.9%	3.7%
Sub-optimal [kW]	13.46	21.67	35.01	49.66	68.59	90.98	118.79
% increase	14.9%	8.0%	2.1%	2.3%	2.5%	3.6%	3.4%

Table 3: Average cycle power production comparison between benchmark, optimal solution, sub-optimal solution.

The results reported in the table 3 show that with respect to the benchmark both the approaches provide a significant improvement of the system performances in terms of average cycle power. The sub-optimal solution results don't show a significant deterioration of the performances. This result suggest that one unique trajectory could be used for the *Transition one* regardless form the wind conditions.

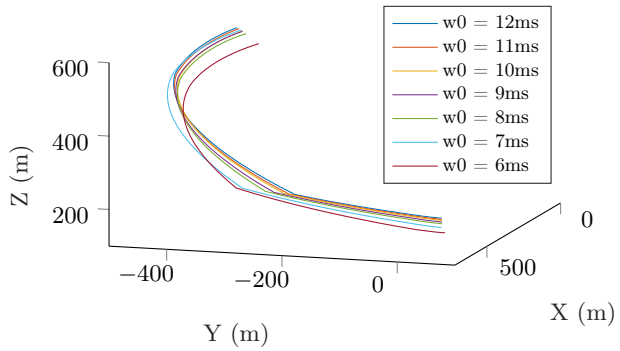

Figure 5: Sub-optimal *Transition 1* trajectory at varying wind speed.

6. Conclusion

The control logic for the *Transition 1* phase developed within this work shows good results in avoiding abrupt increase in the force acting on the tether. This results are obtained with both the implementation and would ensure an higher lifetime of the system components. Moreover the obtained optimal $\theta - \varphi$ trajectory ensure a better efficiency of the overall production cycle. The work also opens several directions for further developments such as the extension of the proposed control logic to the *Transition 2* and the validation of the obtained results with more complex and more realistic wind profiles. If the results obtained in this work were also corroborated by these more complex simulations, it would then be interesting to implement this approach on a real prototype.

References

[1] Andrea Berra and Lorenzo Fagiano. An optimal reeling control strategy for pumping airborne wind energy systems without wind speed feedback. Technical report.

[2] Fagiano Lorenzo Mario. *Control of Tethered Airfoils for High-Altitude Wind Energy Generation*. PhD thesis, Politecnico di Torino, 2009.

[3] Aldo U. Zgraggen, Lorenzo Fagiano, and Manfred Morari. Automatic Retraction and Full-Cycle Operation for a Class of Airborne Wind Energy Generators. *IEEE Transactions on Control Systems Technology*, 24(2):594–608, 3 2016.